Article

Targeted Single-Wall Carbon Nanotube-Mediated Pt(IV) Prodrug Delivery Using Folate as a Homing Device

Shanta Dhar, Zhuang Liu, Ju#rgen Thomale, Hongjie Dai, and Stephen J. Lippard

J. Am. Chem. Soc., **2008**, 130 (34), 11467-11476 • DOI: 10.1021/ja803036e • Publication Date (Web): 29 July 2008

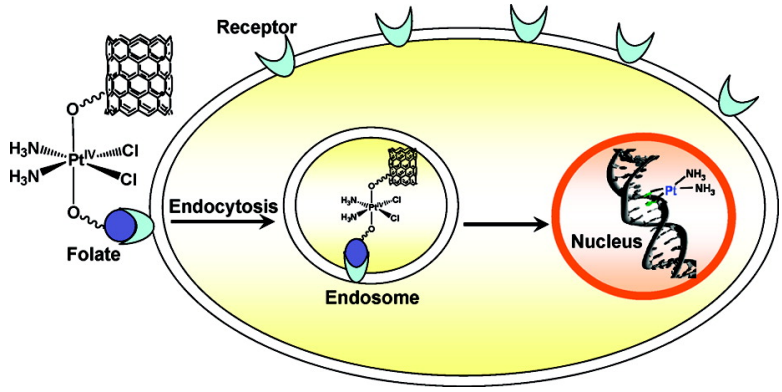

More About This Article

Additional resources and features associated with this article are available within the HTML version:

- Supporting Information
- Access to high resolution figures
- Links to articles and content related to this article
- Copyright permission to reproduce figures and/or text from this article

View the Full Text HTML

J|A|C|S
ARTICLES

Published on Web 07/29/2008

Targeted Single-Wall Carbon Nanotube-Mediated Pt(IV) Prodrug Delivery Using Folate as a Homing Device

Shanta Dhar,[†] Zhuang Liu,[‡] Jürgen Thomale,[§] Hongjie Dai,*[,‡] and Stephen J. Lippard*[,†]

Department of Chemistry, Massachusetts Institute of Technology, Cambridge, Massachusetts 02139, Department of Chemistry and Laboratory for Advanced Materials, Stanford University, Stanford, California 94305, and Institute of Cell Biology, University of Duisburg-Essen, 45122 Essen, Germany

Received April 24, 2008; E-mail: lippard@mit.edu; hdai@stanford.edu

Abstract: Most low-molecular-weight platinum anticancer drugs have short blood circulation times that are reflected in their reduced tumor uptake and intracellular DNA binding. A platinum(IV) complex of the formula *c,c,t*-[$Pt(NH_3)_2Cl_2(O_2CCH_2CH_2CO_2H)(O_2CCH_2CH_2CONH$-PEG-FA)] (**1**), containing a folate derivative (FA) at an axial position, was prepared and characterized. Folic acid offers a means of targeting human cells that highly overexpress the folate receptor (FR). Compound **1** was attached to the surface of an amine-functionalized single-walled carbon nanotube (SWNT-PL-PEG-NH_2) through multiple amide linkages to use the SWNTs as a "longboat delivery system" for the platinum warhead, carrying it to the tumor cell and releasing cisplatin upon intracellular reduction of Pt(IV) to Pt(II). The ability of SWNT tethered **1** to destroy selectively FR(+) vs FR(−) cells demonstrated its ability to target tumor cells that overexpress the FR on their surface. That the SWNTs deliver the folate-bearing Pt(IV) cargos into FR(+) cancer cells by endocytosis was demonstrated by the localization of fluorophore-labeled SWNTs using fluorescence microscopy. Once inside the cell, cisplatin, formed upon reductive release from the longboat oars, enters the nucleus and reacts with its target nuclear DNA, as determined by platinum atomic absorption spectroscopy of cell extracts. Formation of the major cisplatin 1,2-intrastrand d(GpG) cross-links on the nuclear DNA was demonstrated by use of a monoclonal antibody specific for this adduct. The SWNT-tethered compound **1** is the first construct in which both the targeting and delivery moieties have been incorporated into the same molecule; it is also the first demonstration that intracellular reduction of a Pt(IV) prodrug leads to the *cis*-{$Pt((NH_3)_2$} 1,2-intrastrand d(GpG) cross-link in nuclear DNA.

Introduction

In spite of the clinical success of cisplatin (*cis*-dichlorodiammineplatinum(II) or *cis*-DDP),[1–5] there are many occasions when treatment must be discontinued. Drug resistance, acquired and intrinsic, limits the effectiveness of *cis*-DDP and is manifest as reduced cellular uptake, enhanced DNA repair, drug deactivation, or a combination of these mechanisms.

Nanocarriers[6–10] for low-molecular-weight drugs offer a promising strategy for improving body distribution and prolonging blood circulation. Recently, single-walled carbon nanotubes (SWNTs) have been investigated as carriers in living systems.[11–13] They internalize various cargos in cells, including fluoresceins, plasmid DNA, proteins, and other substances that would not otherwise be taken up, with no apparent side effects.[14–16] Well-functionalized nanotubes circulate in the blood with half-lives on the order of a few hours. Nanotube uptake by the reticuloendothelial system (RES) is cleared slowly by the biliary pathway, and the nanotubes end up in feces, without showing obvious toxicity in vivo.[17–19] Because of their extremely low solubility, pristine SWNTs cannot circulate well in biological systems. Their dispersion in biological fluids is achieved by

[†] Massachusetts Institute of Technology.
[‡] Stanford University.
[§] University of Duisburg-Essen.

(1) Rosenberg, B.; VanCamp, L.; Trosko, J. E.; Mansour, V. H. *Nature* **1969**, *222*, 385–386.
(2) Jamieson, E. R.; Lippard, S. J. *Chem. Rev.* **1999**, *99*, 2467–2498.
(3) Wong, E.; Giandomenico, C. M. *Chem. Rev.* **1999**, *99*, 2451–2466.
(4) Galanski, M.; Jakupec, M. A.; Keppler, B. K. *Curr. Med. Chem.* **2005**, *12*, 2075–2094.
(5) Wang, D.; Lippard, S. J. *Nat. Rev. Drug Discovery* **2005**, *4*, 307–320.
(6) Bogunia-Kubik, K.; Sugisaka, M. *Biosystems* **2002**, *65*, 123–138.
(7) Schmidt, J. J.; Montemagno, C. D. *Drug Discovery Today* **2002**, *7*, 500–503.
(8) Roco, M. C. *Curr. Opin. Biotechnol.* **2003**, *14*, 337–346.
(9) Sahoo, S. K.; Labhasetwar, V. *Drug Discovery Today* **2003**, *8*, 1112–1120.
(10) Wilkinson, J. M. *Med. Device Technol.* **2003**, *14*, 29–31.
(11) Kam, N. W. S.; Jessop, T. C.; Wender, P. A.; Dai, H. *J. Am. Chem. Soc.* **2004**, *126*, 6850–6851.
(12) Kam, N. W. S.; Liu, Z.; Dai, H. *J. Am. Chem. Soc.* **2005**, *127*, 12492–12493.
(13) Liu, Z.; Cai, W.; He, L.; Nakayama, N.; Chen, K.; Sun, X.; Chen, X.; Dai, H. *Nat. Nanotechnol.* **2007**, *2*, 47–52.
(14) Liu, Y.; Wu, D.-C.; Zhang, W.-D.; Jiang, X.; He, C.-B.; Chung, T. S.; Goh, S. H.; Leong, K. W. *Angew. Chem., Int. Ed.* **2005**, *44*, 4782–4785.
(15) Bottini, M.; Cerignoli, F.; Dawson, M. I.; Magrini, A.; Rosato, N.; Mustelin, T. *Biomacromolecules* **2006**, *7*, 2259–2263.
(16) Kam, N. W. S.; Liu, Z.; Dai, H. *Angew. Chem., Int. Ed.* **2006**, *45*, 577–581.
(17) Deng, X.; Jia, G.; Wang, H.; Sun, H.; Wang, X.; Yang, S.; Wang, T.; Liu, Y. *Carbon* **2007**, *45*, 1419–1424.

surface functionalization through oxidation, which leaves oxygen-containing functional groups such as alcohols or carboxylic acid, or by the attachment of solubilizing side-chains.[20–25] Once solubilized, SWNTs efficiently cross cell membranes, being taken into the cytosol by endocytosis.[26–28] As a result, various molecules attached to the surface of the SWNT can be internalized. Coupling of macromolecular carriers with a normally endocytosed compound frequently improves its intracellular accumulation.

Recently we demonstrated that functionalized soluble SWNTs can serve as "longboats" to carry Pt(IV) prodrugs into cells through clathrin-dependent endocytosis.[29] The SWNT longboats produce platinum intracellular levels much higher than those for the platinum unit administered in the traditional manner. Efforts to produce potent platinum anticancer drugs have been hindered by their inactivation in the body prior to reaching the tumor. Longboat SWNTs provide an opportunity to shuttle platinum compounds safely through this obstacle course and into the cancer cell.

The SWNT longboats also have the potential to carry additional passengers such as tumor-targeting components to the cancer cell. Targeted drug-delivery systems promise to expand the therapeutic window of platinum complexes, as recently demonstrated for oxaliplatin uptake by colorectal cancer cells via organic cation transporters.[30] Traditional cancer therapy relies on the premise that rapidly proliferating cancer cells are more likely to be killed by a cytotoxic agent. In reality, however, these agents have very little or no specificity, which leads to systemic toxicity, causing undesirable side effects. Therefore, targeted drug-delivery constructs are much desired. In general, a tumor-targeting drug-delivery system consists of a cell surface recognition moiety and a chemical warhead connected directly or through a suitable linker to a delivery system such as a SWNT (Scheme 1). The conjugate itself should be systemically nontoxic, and the linker must be stable in blood circulation. Upon internalization into the cancer cell, the conjugate should be readily cleaved to generate the active agent.

A variety of receptors have been identified as markers for carcinomas. Among these is the folate receptor (α-FR), and its substrate folic acid (FA) has the potential to target several types of cancer cells because of its ability to react with this high-affinity, membrane-anchored protein.[31] Moreover, α-FR is

Scheme 1. Targeted Prodrug-Delivery System

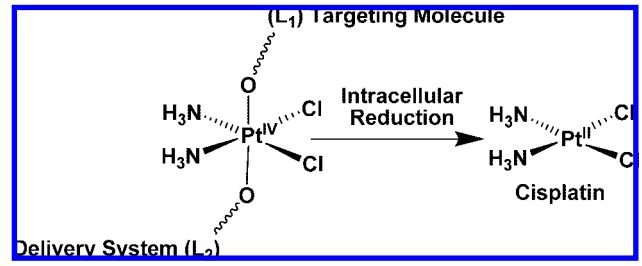

overexpressed by a wide variety of human tumors, including ovarian, endometrial, breast, lung, renal, and colon.[32,33] The highest frequency of α-FR overexpression (>90%) occurs in ovarian carcinomas.[34,35] Expression of α-FR on tumor cell surfaces has led to the exploitation of FA as an important ligand for specific targeting by diagnostic or therapeutic cancer cell agents.[36–39]

Carboplatin, *cis*-[Pt(NH$_3$)$_2$(CBDCA-O,O′)], where CBDCA is cyclobutane-1,1-dicarboxylate, is a second generation platinum anticancer drug widely used for cancer treatment.[40] Carboplatin has a short blood circulation half-life, which reduces tumor uptake and subsequent intracellular DNA binding. Recent efforts to overcome these shortcomings include conjugation of carboplatin, linked to FA by attachment to CBDCA at an equatorial site, to a PEG carrier[41] for folate receptor-mediated endocytosis (FRME).[42,43] The FA−Pt^{II}−PEG conjugates were taken into the cytosol of tumor cells more rapidly than PEG−Pt conjugates, but the latter afforded twice as many Pt−DNA adducts. Apparently, the endocytosed FA−Pt^{II}−PEG conjugate is sequestered in a compartment like the lysosome, where it is separated from the cytosol by a membrane, thereby preventing Pt from reaching its nuclear DNA target.

Platinum(IV) complexes have the potential to overcome these problems. Their octahedral geometry introduces two axial ligands, L_1 and L_2 in Scheme 1, one of which can be attached to a folic acid or other ligand for cellular targeting. The other axial site offers a position for conjugation to a nanocarrier for efficient delivery. Platinum(IV) complexes are prodrugs because they can be reduced in the cytoplasm to unveil an active platinum(II) derivative with concomitant loss of the axial ligands (Scheme 1).[44,45]

(18) Schipper, M. L.; Nakayama-Ratchford, N.; Davis, C. R.; Kam, N. W. S.; Chu, P.; Liu, Z.; Sun, X.; Dai, H.; Gambhir, S. S. *Nat. Nanotechnol.* **2008**, *3*, 216–221.
(19) Liu, Z.; Davis, C.; Cai, W.; He, L.; Chen, X.; Dai, H. *Proc. Natl. Acad. Sci. U.S.A.* **2008**, *105*, 1410–1415.
(20) Qu, L.; Martin, R. B.; Huang, W.; Fu, K.; Zweifel, D.; Lin, Y.; Sun, Y.-P.; Bunker, C. E.; Harruff, B. A.; Gord, J. R.; Allard, L. F. *J. Chem. Phys.* **2002**, *117*, 8089–8094.
(21) Georgakilas, V.; Kordatos, K.; Prato, M.; Guldi, D. M.; Holzinger, M.; Hirsch, A. *J. Am. Chem. Soc.* **2002**, *124*, 760–761.
(22) Hirsch, A. *Angew. Chem., Int. Ed* **2002**, *41*, 1853–1859.
(23) Holzinger, M.; Abraham, J.; Whelan, P.; Graupner, R.; Ley, L.; Hennrich, F.; Kappes, M.; Hirsch, A. *J. Am. Chem. Soc.* **2003**, *125*, 8566–8580.
(24) Hirsch, A.; Vostrowsky, O. *Top. Curr. Chem.* **2005**, *245*, 193–237.
(25) Prato, M.; Kostarelos, K.; Bianco, A. *Acc. Chem. Res.* **2008**, *41*, 60–68.
(26) Kam, N. W. S.; Dai, H. *J. Am. Chem. Soc.* **2005**, *127*, 6021–6026.
(27) Kam, N. W. S.; O'Connell, M.; Wisdom, J. A.; Dai, H. *Proc. Natl. Acad. Sci. U.S.A.* **2005**, *102*, 11600–11605.
(28) Gao, L.; Nie, L.; Wang, T.; Qin, Y.; Guo, Z.; Yang, D.; Yan, X. *ChemBioChem* **2006**, *7*, 239–242.
(29) Feazell, R. P.; Nakayama-Ratchford, N.; Dai, H.; Lippard, S. J. *J. Am. Chem. Soc.* **2007**, *129*, 8438–8439.
(30) Zhang, S.; Lovejoy, K.; Shima, J. E.; Lagpacan, L. L.; Shu, Y.; Lapuk, A.; Gray, J. W.; Chen, X.; Lippard, S. J.; Giacomini, K. M. *Cancer Res.* **2006**, *66*, 88847–88857.
(31) Antony, A. C. *Blood* **1992**, *79*, 2807–2820.
(32) Weitman, S. D.; Lark, R. H.; Coney, L. R.; Fort, D. W.; Frasca, V.; Zurawski, V. R., Jr.; Kamen, B. A. *Cancer Res.* **1992**, *52*, 3396–3401.
(33) Ross, J. F.; Chaudhuri, P. K.; Ratnam, M. *Cancer* **1994**, *73*, 2432–2443.
(34) Garin-Chesa, P.; Campbell, I.; Saigo, P. E.; Lewis, J. L., Jr.; Old, L. J.; Rettig, W. J. *Am. J. Pathol.* **1993**, *142*, 557–567.
(35) Parker, N.; Turk, M. J.; Westrick, E.; Lewis, J. D.; Low, P. S.; Leamon, C. P. *Anal. Biochem.* **2005**, *338*, 284–293.
(36) Bae, Y.; Jang, W.-D.; Nishiyama, N.; Fukushima, S.; Kataoka, K. *Mol. BioSyst.* **2005**, *1*, 242–250.
(37) Mueller, C.; Schubiger, P. A.; Schibli, R. *Eur. J. Nucl. Med. Mol. Imaging* **2006**, *33*, 1162–1170.
(38) Mueller, C.; Schubiger, P. A.; Schibli, R. *Bioconjugate Chem.* **2006**, *17*, 797–806.
(39) Zhang, Z.; Lee, S. H.; Feng, S.-S. *Biomaterials* **2007**, *28*, 1889–1899.
(40) Harrap, K. R. *Cancer Res.* **1995**, *55*, 2761–2768.
(41) Aronov, O.; Horowitz, A. T.; Gabizon, A.; Gibson, D. *Bioconjugate Chem.* **2003**, *14*, 563–574.
(42) Wang, S.; Low, P. S. *J. Controlled Release* **1998**, *53*, 39–48.
(43) Sudimack, J.; Lee, R. J. *Adv. Drug Delivery Rev.* **2000**, *41*, 147–162.
(44) Barnes, K. R.; Kutikov, A.; Lippard, S. J. *Chem. Biol.* **2004**, *11*, 557–564.
(45) Mukhopadhyay, S.; Barnes, C. M.; Haskel, A.; Short, S. M.; Barnes, K. R.; Lippard, S. J. *Bioconjugate Chem.* **2008**, *19*, 39–49.

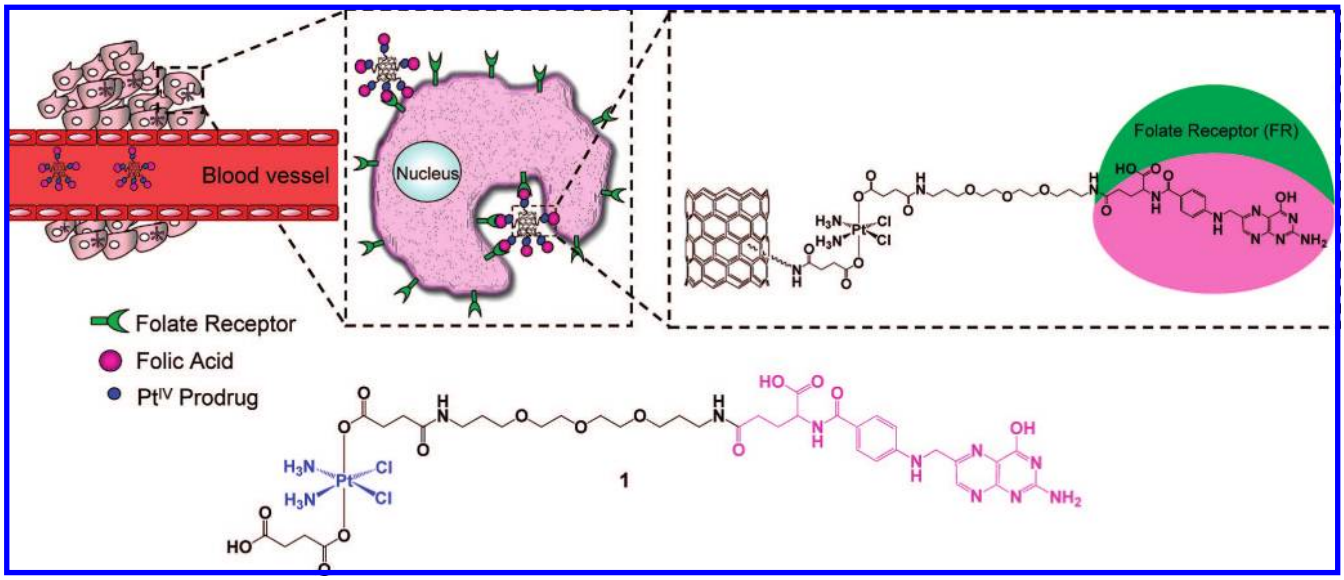

Figure 1. Folate receptor (FR)-mediated targeting and SWNT-mediated delivery of **1** by endocytosis and structure of **1**.

The goal of the present study was to utilize the targeting properties of folic acid with the delivery feature of SWNTs to develop a Pt(IV)−SWNT longboat for targeting delivery of *cis*-DDP upon reduction in the cell (Scheme 1). We therefore designed a Pt(IV) complex *c*,*c*,*t*-[$Pt(NH_3)_2Cl_2(O_2CCH_2CH_2CO_2H)(O_2CCH_2CH_2CONH$-PEG-FA)] (**1**, Figure 1), having succinate as one of its axial ligands for conjugation with amine-functionalized SWNTs.[29] The second axial ligand contains a folic acid derivative separated from the platinum center by a PEG spacer. The use of PEG makes the compound more water soluble and biocompatible.[46]

Experimental Section

Materials and Measurements. The complexes *cis*-[$Pt(NH_3)_2Cl_2$],[47] *c*,*c*,*t*-[$Pt(NH_3)_2Cl_2(OH)_2$],[48] *c*,*c*,*t*-[$Pt(NH_3)_2Cl_2(O_2CCH_2CH_2CO_2H)_2$],[44] and 6-carboxy-2′,7′-dichlorofluorescein-3′,6′-diacetate succinimidyl ester[49] were synthesized as previously described. SWNTs made by a high-pressure CO (Hipco) method were purchased and used to construct amine-functionalized SWNTs via nonspecific interactions between the SWNT surface and an amine-terminated PEGylated phospholipid (PL-PEG-NH_2).[13] Distilled water was purified by passage through a Millipore Milli-Q Biocel water purification system (18.2 MΩ) with a 0.22 μm filter. *N*-Hydroxysuccinimide (NHS), 1-ethyl-3-[3-dimethylaminopropyl]-carbodiimide hydrochloride (EDC), paraformaldehyde, *N*,*N*-diisopropylethylamine (DIPEA), hydroxyethyl starch (HAES), and succinic anhydride were purchased from Aldrich. 2-(1*H*-7-azabenzotriazol-1-yl)-1,1,3,3-tetramethyluronium hexafluorophosphate methanaminium (HATU) was purchased from Applied Biosystems. A monoclonal cisplatin 1,2-d(GpG) intrastrand cross-link specific antibody R-C18 was synthesized as previously reported.[50] FITC-labeled secondary antibody rabbit anti(rat Ig) was obtained from Invitrogen. Specific adhesion slides for immunofluoresecence were purchased from Squarix Biotechnology (Marl, Germany). All other solvents and reagents were obtained from VWR International and used as received. ^{1}H NMR and ^{195}Pt NMR spectra were recorded on a Bruker AVANCE-400 NMR spectrometer with a Spectro Spin superconducting magnet in the Massachusetts Institute of Technology Department of Chemistry Instrumentation Facility (MIT DCIF). Atomic absorption spectroscopic measurements were taken on a Perkin-Elmer AAnalyst 300 spectrometer. LC-MS analyses were performed on an Agilent 1100 series instrument. HPLC analyses were carried out using an Agilent 1200 series instrument. HRMS analyses were performed on a Bruker Daltonics APEXIV 4.7 T Fourier transform ion cyclotron resonance mass spectrometer in the MIT DCIF. Electrochemical measurements were made at 25 °C on a 263 EG&G Princeton Applied Research electrochemical analyzer with electrochemical analysis software 270 for voltammetric work using a three-electrode setup comprising a glassy carbon working electrode, a platinum wire auxiliary electrode, and a Ag/AgCl reference electrode. The electrochemical data were uncorrected for junction potentials. KCl was used as supporting electrolyte. Fluorescence imaging studies were performed with an Axiovert 200 M inverted epifluorescence microscope (Zeiss, Thornwood, NY) equipped with an EM-CCD digital camera C9100 (Hamamatsu, Japan). An X-Cite 120 metal halide lamp (EXFO, Quebec, Canada) was used as the light source. The microscope was operated with Volocity software (Improvision, Lexington, MA).

Synthesis of $H_2N(CH_2)_3O(CH_2)_2O(CH_2)_2O(CH_2)_3NHBOC$ (3). A solution of 4,7,10-trioxa-1,13-tridecanediamine (7.5 g, 34.1 mmol) in 1,4-dioxane (100 mL) was treated with BOC-anhydride (3.7 g, 16.9 mL). The mixture was stirred at room temperature for 12 h. The solvent was removed, and the resulting yellow oil was purified by silica gel flash chromatography (2−10% MeOH in CH_2Cl_2) to produce the oil **3** in 49% (5.5 g) yield. ^{1}H NMR ($CDCl_3$): δ 5.1 (s, 1H), 3.58−3.50 (m, 12H), 3.21 (d, J = 6.9 Hz, 2H), 2.79 (t, J = 8 Hz, 2H), 1.75−1.69 (m, 4H), 1.59 (s, 2H), 1.42 (s, 9H). ^{13}C NMR ($CDCl_3$): δ 155.0, 69.2, 68.9, 66.7, 48.0, 37.6, 30.4, 28.6, 27.3. HRMS-ESI: calcd = 321.2384 for $[M + H]^+$, found = 321.2372.

Synthesis of 4. Folic acid (1 g, 2.26 mmol) was dissolved in 20 mL of dry dimethylformamide (DMF) to which 0.31 g (1.52 mmol) of dicyclohexylcarbodiimide (DCC) and 0.257 g (2.26 mmol) of NHS were added. The reaction mixture was stirred for 14 h at room temperature in the dark. The byproduct, dicyclohexylurea, was filtered off, and 100 mL of 30% acetone in diethyl ether was added with stirring. A yellow precipitate formed and was collected on a sintered glass crucible; after washing with acetone and ether several

(46) Zalipsky, S. *Adv. Drug Delivery Rev.* **1995**, *16*, 157–182.
(47) Dhara, S. C. *Indian J. Chem.* **1970**, *8*, 193–194.
(48) Hall, M. D.; Dillon, C. T.; Zhang, M.; Beale, P.; Cai, Z.; Lai, B.; Stampfl, A. P. J.; Hambley, T. W. *J. Biol. Inorg. Chem.* **2003**, *8*, 726–732.
(49) Woodroofe, C. C.; Won, A. C.; Lippard, S. J. *Inorg. Chem.* **2005**, *44*, 3112–3120.
(50) Liedert, B.; Pluim, D.; Schellens, J.; Thomale, J. *Nucleic Acids Res.* **2006**, *34*, e47.

Scheme 2. Synthetic Route to **1**

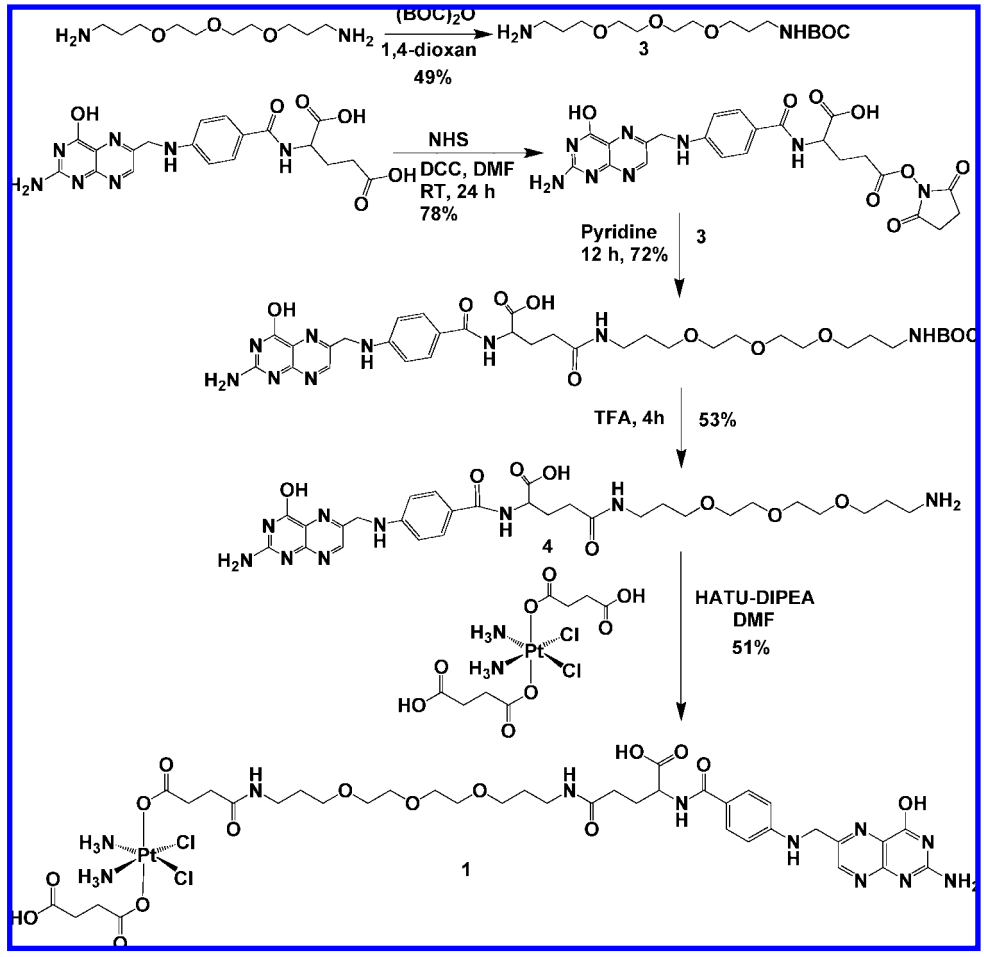

Scheme 3. Synthetic Procedure for Synthesizing **2**

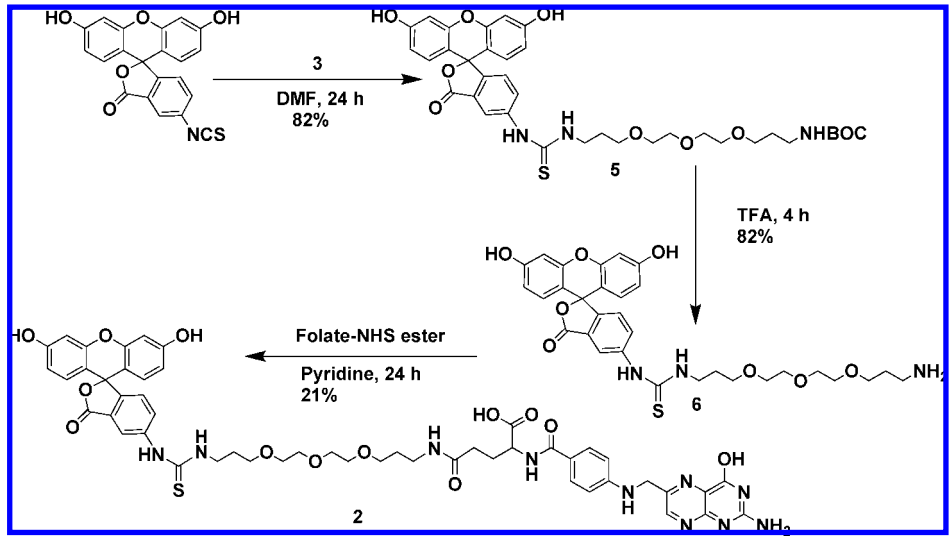

times, the material was used immediately for the next step in the synthesis. Folate-NHS ester (1.2 g, 2.2 mmol) was dissolved completely in 100 mL of dry pyridine, and **3** (0.73 g, 2.27 mmol) was slowly added over 30 min. The mixture was stirred at room temperature in the dark for 12 h. After pyridine was evaporated, the resulting compound was dissolved in 5 mL of trifluoroacetic acid (TFA) to remove the BOC group. Deprotection was carried out at room temperature for 4 h. TFA was removed under vacuum. The resulting compound was loaded onto a DEAE Sephadex A25 column packed with potassium tetraborate, and the compound was eluted with 10−50 mM ammonium bicarbonate. Fractions were collected and lyophilized. Compound **4** was isolated in 53% (1.24 g) yield. ^{1}H NMR (DMSO-d_6): δ 8.67 (s, 1H), 7.86−7.64 (m, 6H), 6.64 (d, J = 8 Hz, 2H), 4.5 (s, 2H), 4.33−4.26 (m, 1H), 3.6−3.3 (m, 14H), 3.07 (d, J = 4 Hz, 2H), 2.88−2.82 (m, 2H), 2.49 (s, 2H), 2.36−2.15 (m, 2H), 1.76 (t, J = 4 Hz, 2H), 1.61−0.99 (m, 4H). ^{13}C NMR (DMSO-d_6): δ 174.4, 172.1, 166.5, 160.8, 158.5, 153.3, 151.0, 148.3, 129.4, 128.3, 121.4, 111.2, 69.7, 69.6, 69.5,

Scheme 4. Synthetic Procedure for Synthesizing SWNT−**1**

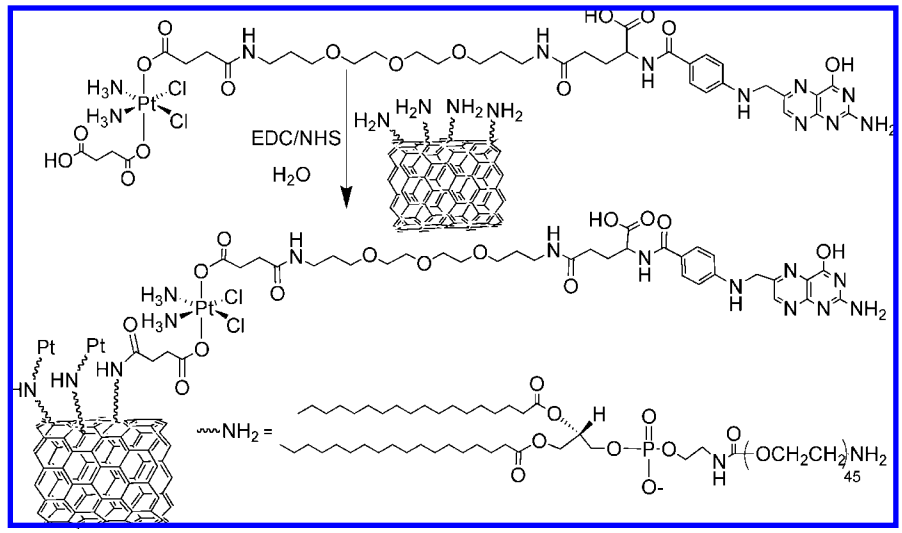

Table 1. Comparison of Reduction Potentials for Pt(IV) Compounds

complex[a]	reduction potential (mV) at pH 7.4 vs NHE	ref
$[Pt(en)(OCOCF_3)_2Cl_2]$	197	58
$[Pt(dach)Cl_4]$	107	58
$[Pt(a,cha)(OCOC_3H_7)_2Cl_2]$	47	58
$[Pt(en)Cl_4]$	37	58
$[Pt(a,cha)(OCOCH_3)_2Cl_2]$	−53	58
$[Pt(en)(OCOCH_3)_2Cl_2]$	−349	59
$[Pt(ipa)(OH)_2Cl_2]$	−533	58
$[Pt(en)(OH)_2Cl_2]$	−687	59
1	−698	this work

[a] en = ethylenediamine; ipa = isopropylamine; a = amine; cha = cyclohexylamine; dach = diaminocyclohexane.

68.0, 67.4, 46.2, 36.9, 35.6, 30.6, 29.3, 27.2. HRMS-ESI: calcd = 644.3151 for $[M + H]^+$, found = 644.3140.

Synthesis of *c,c,t*-[Pt(NH$_3$)$_2$Cl$_2$(O$_2$CCH$_2$CH$_2$CO$_2$H)(O$_2$CCH$_2$CH$_2$CONH-PEG-FA)] (1). To a solution of *c,c,t*-[Pt(NH$_3$)$_2$Cl$_2$(O$_2$CCH$_2$CH$_2$CO$_2$H)$_2$] (0.2 g, 0.38 mmol) in DMF (10 mL) was added a DMF solution (0.5 mL) containing HATU (0.217 g, 0.57 mmol). This mixture was stirred for 10 min at room temperature. To the resulting solution was added a DMF solution containing **4** (0.193 g, 0.3 mmol) and DIPEA (0.056 g, 0.432 mmol). The mixture was stirred at room temperature for 24 h in the dark. The DMF was then removed under vacuum to afford a yellow oil. Diethyl ether was added to precipitate a yellow solid, **1**. Compound **1** was purified by reprecipitation, first dissolving it in MeOH and then adding diethyl ether. As a final purification, **1** was repeatedly washed with acetone and then isolated as a yellow solid in 51% (0.2 g) yield. IR (KBr): ν_{max} 3382, 2922, 1700, 1684, 1662, 1607, 1558, 1539, 1506, 1301, 1261, 1189, 1100, 846, 667, 558 cm^{-1}. ^{1}H NMR (DMSO-d_6): δ 8.6 [s, 1H (=NCH)], 7.9−7.7 [b, 2H (NH_2)], 7.7−7.5 [b, 2H (Ar)], 6.9 [b, 2H (NH)], 6.6 [b, 2H (Ar)], 6.5 [b, 6H (NH_3)], 4.44 [d, J = 5.6 Hz, 2H ($NHCH_2$)] 3.7−3.4 [m, 12H (OCH_2)], 3.15−2.91 [m, 4H ($NHCH_2$)], 2.65−2.1 [m, 10H (NCH_2 and CH_2)], 1.55 [t, J = 6.4 Hz, 6H (CH_2 and $C(O)CH_2$)] (Figure S1, Supporting Information). ^{195}Pt NMR (DMSO-d_6): δ = 1220.79 (Figure S2). Mp (decomposition): 167−170 °C. ESI-MS (−): calcd = 1158.28 for $[M - H]^-$, found = 1158.10 (Figure S3).

Synthesis of 5. Fluorescein isothiocyanate (FITC, 0.25 g, 0.64 mmol) was dissolved in dry DMF (2 mL) and **3** (0.266 g, 0.832 mmol) was added. The reaction mixture was stirred at room temperature for 24 h. DMF was removed under vacuum. The residue was purified by silica flash chromatography (5−15% MeOH in $CHCl_3$) to produce **5** in 82% (0.44 g) yield. ^{1}H NMR (CD_3OD): δ 7.98 (s, 1H), 7.05 (d, J = 8 Hz, 1H), 6.55 (t, J = 4 Hz, 1H), 6.43 (s, 4H), 6.41 (t, J = 8 Hz, 2H), 3.51 (s, 2H), 3.50−3.34 (m, 12H), 2.99 (d, J = 4 Hz, 2H), 1.81 (t, J = 4 Hz, 2H), 1.57 (t, J = 4 Hz, 2H), 1.29 (s, 9H). ^{13}C NMR (CD_3OD): δ 171.3, 161.5, 158.6, 154.3, 142.5, 130.5, 125.9, 113.8, 111.6, 103.7, 80.1, 79.7, 71.6, 71.5, 71.3, 71.2, 70.6, 70.0, 49.8, 48.5, 44.0, 38.8, 31.0, 29.9, 28.9. ESI-MS (−): calcd = 708.26 for $[M - H]^-$, found = 708.20.

Synthesis of 6. To a solution of **5** (0.4 g, 0.56 mmol) in CH_2Cl_2 (2 mL) was added TFA (5 mL) at 0 °C. The mixture was stirred for 4 h at room temperature. The solvent was evaporated, the oily residue was dissolved in MeOH, and **6** was precipitated as a yellow solid by addition of excess diethyl ether. The solid was washed with diethyl ether several times and dried in vacuo. Compound **6** was isolated in 82% (0.28 g) yield. ^{1}H NMR (CD_3OD): δ 8.14 (s, 1H), 7.72 (dd, J = 1.92 and 8.3 Hz, 1H), 7.09 (d, J = 8 Hz, 1H), 6.95 (d, J = 8.8 Hz, 2H), 6.81 (d, J = 2 Hz, 2H), 6.68−6.66 (m, 2H), 3.55 (m, 2H), 3.49−3.41 (m, 12H), 2.89 (t, J = 6.6 Hz, 2H), 1.79−1.69 (m, 4H). ^{13}C NMR (CD_3OD): δ 181.6, 173.7, 160.4, 159.1, 158.7, 132.7, 132.5, 132.0, 131.5, 130.1, 124.1, 104.4, 80.2, 71.4, 71.3, 71.2, 70.4, 67.0, 44.3, 39.9, 30.0, 28.4. ESI-MS (+): calcd = 610.22 for $[M + H]^+$, found = 610.1.

Synthesis of 2. Compound **6** (60 mg, 0.098 mmol) was added to a solution of folate-NHS ester (54 mg, 0.098 mmol) in pyridine (1 mL) and the mixture was stirred for 24 h at room temperature in the dark. After evaporation of pyridine, the residue obtained was purified by reverse-phase HPLC (Figure S4) using a C-18 column to produce **2** in 21% (23 mg) yield. ESI-MS (−): calcd = 1031.34 for $[M - H]^-$, found = 1031.5 (Figure S5). HRMS-ESI: calcd = 1055.3328 for $[M + Na]^+$, found = 1055.3343.

Synthesis of SWNT-PL-PEG-NH$_2$. SWNTs functionalized with phospholipid (PL) polyethylene glycol (PEG)-linked amines (SWNT-PL-PEG-NH_2) were prepared by a known procedure.[13] Briefly, raw Hipco SWNTs were sonicated in PL-PEG-NH_2 for 1 h, followed by centrifugation (2.4×10^4 g, 6 h) to remove catalysts and large aggregates. Excess free PL-PEG-NH_2 was removed from the supernatant by ultrafiltration using 100 kDa Millipore filters. The resulting solution contained SWNTs with an average length of about 200 nm, as determined by atomic force microscopy. The molar concentration of the functionalized SWNTs was computed by measuring the absorption at 808 nm ($\varepsilon = 7.9 \times 10^6$ M^{-1} cm^{-1}). The number of amine groups on each nanotube was estimated to be between 50 and 100.

Synthesis of SWNT−Pt(IV) Conjugates. The synthesis of SWNT−Pt(IV) conjugates was carried out by using standard amide coupling reactions. In a typical reaction, a 1.0 mM aqueous solution of NHS (20 μL) was added to an equal volume of an aqueous 1.0 mM solution of EDC, and the resulting solution was allowed to

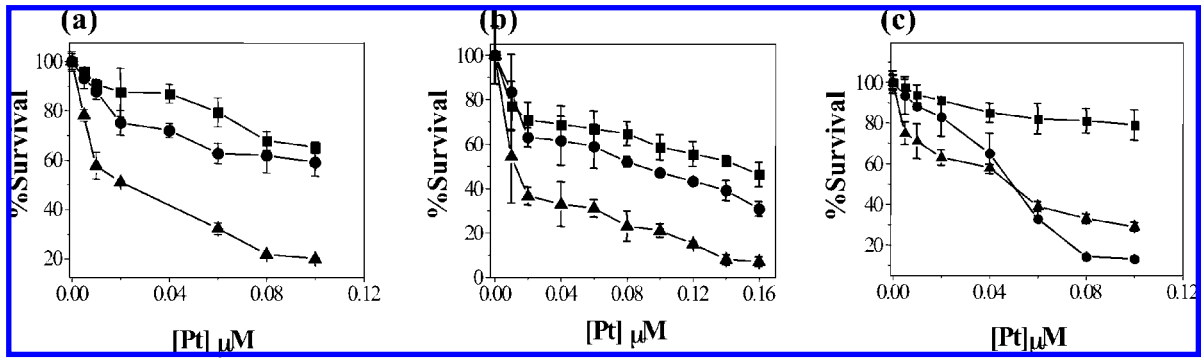

Figure 2. Survival of (a) FR(+) JAR, (b) FR(+) KB, and (c) FR(−) NTera-2 cells treated with **1** (■), SWNT−**1** (▲), or cisplatin (●).

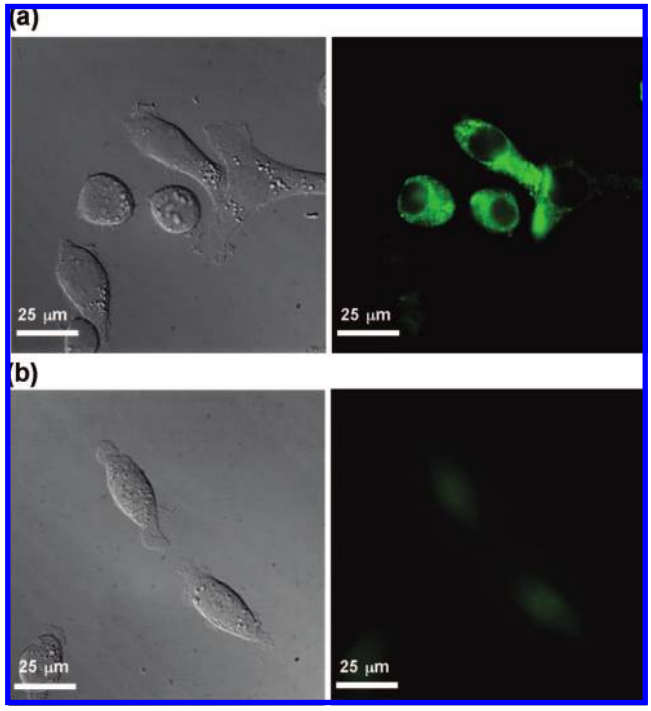

Figure 3. Fluorescence of **2** in (a) FR(+) KB and (b) FR(−) NTera-2 cells.

stand at room temperature for 10 min. To this solution was added 0.8 mol equiv of compound **1** in ddH_2O (40 μL). After 10 min, a solution of SWNT-PL-PEG-NH_2 was added; the mole ratio of amine to Pt was 0.5. The solution was heated to 50 °C for 2 h and then stirred for 12 h at room temperature. The solution was dialyzed against deionized water in a 3500 MW cutoff dialysis cassette for 10 h, changing the water at 5 h. The concentration of SWNT−Pt(IV) was subsequently determined by platinum AAS.

Synthesis of SWNT−Pt(IV)−Fl Conjugates. Following the procedure mentioned above, SWNT−Pt(IV) conjugates with an amine-to-Pt ratio of 2:1 were prepared. These conjugates were then allowed to react with a 0.4 mM aqueous solution of 6-carboxy-2′,7′-dichlorofluorescein-3′,6′-diacetate succinimidyl ester for 12 h at room temperature. The resulting solution was dialyzed against water using a 3500 MW cutoff dialysis cassette for 12 h, and the platinum concentration was determined by AAS.

HPLC Monitoring of Carboxypeptidase-G (CPG)-Mediated Cleavage of 4. Carboxypeptidase-G_2 (CPG) digestion was followed by using reverse-phase HPLC. An analytical (VYDAC) C18 column was used at a flow rate of 1 mL/min, monitoring absorbance at a wavelength of 285 nm. A solution of **4** (155 μM) was prepared in 150 mM Tris buffer (pH 7.3). An aliquot of this solution was injected into the HPLC system to obtain the time zero peak intensity. To this solution was added carboxypeptidase G (CPG, Sigma, 1 unit), and the resulting solution was incubated at 30 °C for 24 h. The solution was then analyzed by HPLC after 24 h.

Electrochemical Studies of Platinum(IV) Compounds. The platinum(IV) complex **1** was dissolved to a final concentration of 2.0 mM in 0.1 M aqueous KCl buffered with phosphate to either pH 6.0 or 7.4. Cylic voltammetric (CV) measurements were carried out at varying scan rates of 50−300 mV s^{-1}. The solvent was degassed by several freeze−pump−thaw cycles, and measurements were taken under an atmosphere of argon.

Cell Culture. a. Medium. Cells were cultured in FA-free RPMI medium (RPMI-1640, Invitrogen) with 10% fetal bovine serum, 2 mM glutamine, 50 units/mL penicillin, and 50 μg/mL streptomycin. The concentration of FA in serum-containing FA-free medium is only 3 nM, as opposed to 2.26 μM (1 mg/L) under normal culture conditions. Cells were routinely passed by treatment with trypsin (0.05%)/EDTA.

b. Cell Lines. Human nasopharyngeal epidermoid carcinoma (KB), choriocarcinoma (JAR), and human testicular cancer (NTera-2) cells were cultured in FA-free RPMI for several passages. Cells were passed every 3−4 days and reseeded from frozen stocks after reaching passage number 20.

MTT Cell Proliferation Assay. KB, JAR, or NTera-2 cells were seeded in 96-well tissue culture plates and maintained overnight in RPMI medium. Cells were then treated with various concentrations of **1**, SWNT−**1**, or *cis*-DDP at different concentrations. The plates were incubated for 72 h at 37 °C. The cells were then treated with 20 μL of 3-(4,5-dimethylthiazol-2-yl)-2,5-diphenyltetrazolium bromide (MTT, 5 mg/mL in PBS) and incubated for 5 h. The medium was removed, the cells were lysed by adding 100 μL of DMSO, and the absorbance of the purple formazan was recorded at 550 nm using a Spectra MAX 340PC plate reader.

Cell Fixing Solution. Paraformaldehyde (4.0 g) and NaOH (0.4 g) were dissolved in 100 mL of distilled water. To this solution was added NaH_2PO_4 (1.68 g), and the pH was adjusted to be in the range 7.5−8.0 by adding NaOH.

Fluorescence Sample Mounting Media. For sample mounting, a solution containing 20 mM Tris (pH 8.0), 0.5% *N*-propyl gallate, and 50−90% glycerol was used.

Fluorescence Microscopy Experiments on KB and NTera-2 Cells. KB or NTera-2 cells were seeded on microscope coverslips (1 cm) at a confluence of 1600 cells per slip and incubated overnight at 37 °C in FA-free RPMI. The medium was changed, and SWNT−Pt(IV)−Fl or **2** was added to a final fluorophore concentration of 1.0 μM. The cells were incubated for 2.5 h at 37 °C. RPMI was then removed, and the cells were incubated with fixing solution for 1 h at room temperature, followed by three washes with phosphate-buffered saline (PBS, pH 7.4). Cells were then permeabilized with 0.1% Triton-X 100 in PBS for 10 min, followed by five washes using PBS. Cells were treated with a PBS solution of

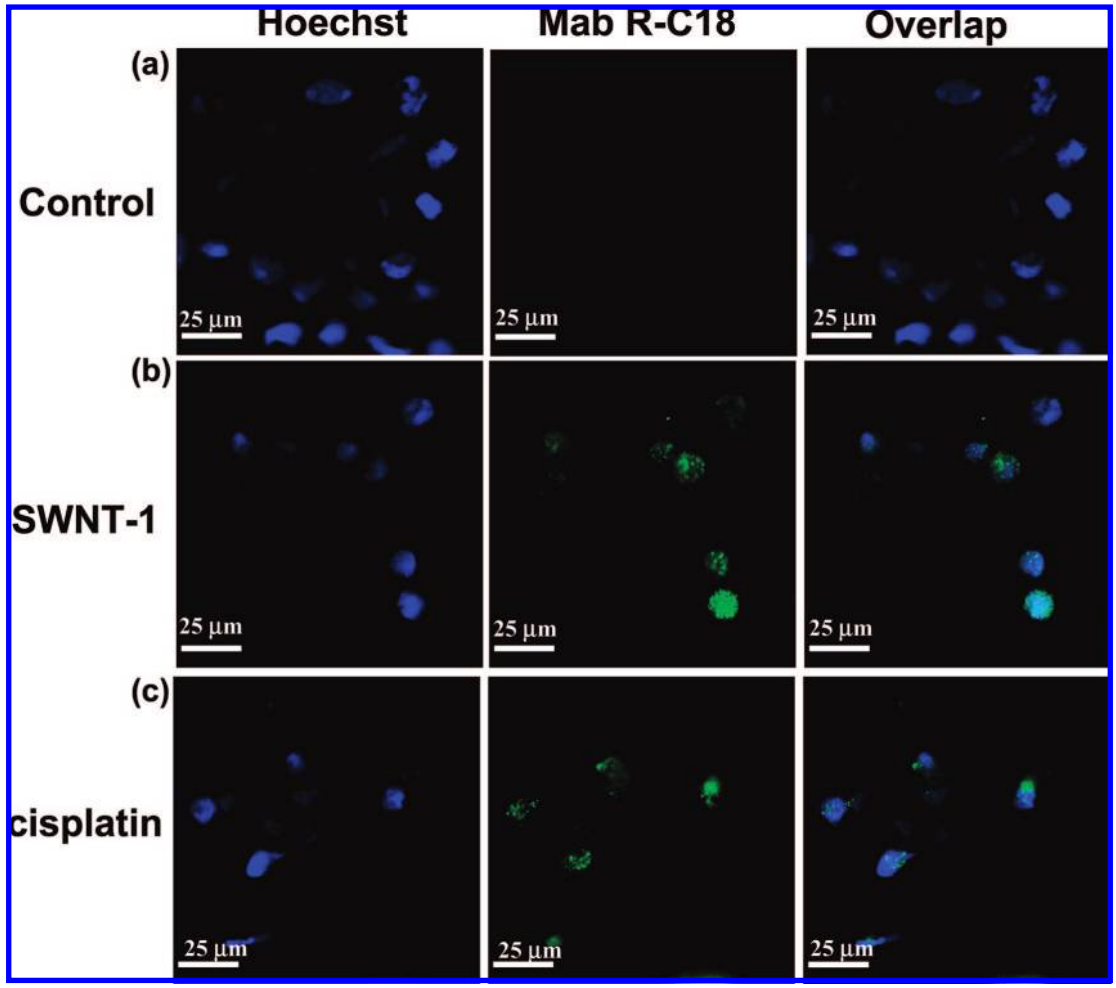

Figure 4. Visualization of Pt−1,2-d(GpG) intrastrand cross-links in the nuclear DNA of KB cells after treatment with (b) SWNT−**1** and (c) *cis*-DDP. (a) Immunofluorescence of untreated KB cells. Nuclei were stained with Hoechst (blue), and Pt−1,2-d(GpG) in DNA were visualized using Mab R-C18 (green).

Hoechst H33258 (250 μg/L) for 10 min at room temperature for nuclear staining. The cells were then washed three times with PBS, followed by two washes using Millipore water. They were mounted on microscope slides using the mounting solution for imaging. Images were collected at 500 ms for the DAPI channel and 270 ms for the FITC channel.

Determination of Platinum Concentrations from Cell Extracts. KB cells were grown in FA-free RPMI to >95% confluence in 175 cm^2 flasks. These cells were then treated either with 1 μM **1** or SWNT−**1** and subsequently incubated for 3 h at 37 °C. Cells were washed with PBS three times and released by trypsinization into PBS. Solutions containing cells were then centrifuged at 800*g* for 10 min, and the cell pellet obtained was resuspended in 100 μL of ice-cold lysis buffer (1.0 mM DTT, 1.0 mM PMSF, 10 mM KCl, 10 mM $MgCl_2$, pH 7.5) for 15 min. This process was repeated, and finally the pellets were resuspended in 40 μL of ice-cold lysis buffer. The cell membranes were lysed by 10 strokes of a 28 ga. syringe. The resulting suspension was centrifuged at 11000*g* for 20 min, and the cytosolic fraction of the cells was collected as supernatant. The pellet was resuspended in 40 μL of extraction buffer (1.0 mM DTT, 1.0 mM PMSF, 1.5 mM $MgCl_2$, 0.2 M EDTA, 0.42 M NaCl, 25% glycerol, pH 7.9) and lysed with 10 strokes of a 28 ga. syringe. The lysate was shaken at 1000 rpm for 45 min at 4 °C and then centrifuged at 20000*g* for 10 min at 4 °C. The supernatant was collected as the nuclear fraction. Platinum concentrations in all the fractions were determined by AAS. The protein concentration in each fraction was determined by using bicinchoninic acid (BCA) assay. Total platinum concentrations were expressed as nanograms of Pt per microgram of protein.

Immunofluorescence for Platinum 1,2-d(GpG) Intrastrand Cross-Link Detection. KB cells were cultured in a six-well plate in folate-free RPMI and treated with SWNT−Pt(IV) or *cis*-DDP at a concentration of 1 μM for 12 h. The cells were released by trypsinization and washed with medium followed by PBS. The cells were then resuspended in HAES−sterile PBS at a density of 1×10^6 per mL. A 10 μL portion of the cell solution was placed onto a precoated slide (ImmunoSelect, Squarix) and air-dried. The cells were then fixed using methanol at −20 °C for 45 min. Samples were washed two times with PBS. Alkali denaturation of nuclear DNA was then performed by using a solution of 60% 70 mM NaOH/140 mM NaCl−40% MeOH at 0 °C for 5 min. After two washes with PBS, removal of cellular proteins was carried out by digestion with pepsin (30 μg/mL) for 10 min at 37 °C, followed by treatment with proteinase K (6 μg/mL) for 10 min at 37 °C in a humid chamber. The cells were washed with PBS−0.2% glycin. After blocking with milk (5% in PBS) for 30 min at room temperature, cells were incubated with anti-Pt-1,2-d(GpG) antibody R-C18[50] (0.2 μg/mL) at 4 °C for 12 h in a humid chamber. The cells were then washed with PBS three times. After blocking with milk for 30 min at room temperature, cells were incubated with FITC-labeled rabbit anti(rat Ig) secondary antibody at 37 °C for 1 h. After three washes with PBS, the cells were treated with a PBS solution of Hoechst H33258 (250 μg/L) for 10 min at room

temperature for nuclear staining. The cells were then washed three times with PBS and mounted using the mounting solution for imaging.

Results and Discussion

Synthesis and Chemical Characterization. The molecular design of the Pt(IV) compound **1**, containing both a folate derivative and a succinate with a free carboxylic (Figure 1), was inspired by the asymmetric Pt(IV) compound [$Pt(NH_3)Cl_2(OEt)(O_2CCH_2CH_2CO_2H)$] recently reported by us.[29] The folic acid derivative **4** (Scheme 2) was designed such that the basic requirements for interaction with the folate receptor were maintained. Folic acid contains two carboxylate groups that can be used for conjugation to the Pt(IV) center. Modification of the γ carboxylate group allows conjugation without significant loss of binding affinity for the folate receptor. Folic acid was therefore derivatized at the γ position with a polyethylene glycol (PEG) spacer. Efficient FR binding can be achieved by separating the folate from the Pt(IV) center by a PEG spacer. The mono-BOC-protected PEG-amine was prepared by a standard procedure using 4,7,10-trioxa-1,13-tridecanediamine. The synthesis of the folate-γ-NHS ester, illustrated in Scheme 2, was carried out by the procedure reported earlier.[51]

The BOC-protected folate-PEG-amine was synthesized by reacting mono-BOC-protected PEG-amine (**3**) with NHS-folate, as indicated in Scheme 2. A ninhydrin assay was used to follow the progress of the reaction. Folate-PEG-amine (**4**) was released by a standard BOC deprotection method in the final step.

The isomeric purity of **4** is an important issue for binding to the FR. We used a carboxypeptidase G2 (CPG)-digestion assay[52] to measure the percent of γ-isomer in the folate-PEG-amine **4**. CPG is a lysosomal, thiol-dependent protease that hydrolyzes only γ-amides but not the α-isomer.[53] Derivatization of the α-carboxyl group of folate prevents hydrolysis by CPG, but derivatization of the γ-carboxyl has little effect on the enzyme activity. A solution of **4** (155 μM) in 150 mM Tris buffer (pH 7.3) shows two peaks (Figure S6a) under HPLC conditions, both giving rise to an *m*/*z* peak at 644.3 in their LC-MS spectra. The assignment of the structures of the two isomers of folate-PEG-amine was carried out by CPG hydrolysis. When a solution of **4** (155 μM) in 150 mM Tris buffer (pH 7.3) was tested as a substrate for the CPG enzyme, the minor peak at 11.0 min was unchanged, while the peak at 13.5 min revealed hydrolysis (Figure S6b). This experiment showed that >90% of the FA residues in conjugate **4** are γ-carboxyl-linked. HPLC chromatograms of compound **4** before and after treatment with CPG are available in Figures S6a and S6b, respectively.

cis,*trans*,*cis*-[$Pt(NH_3)_2(succinate)_2Cl_2$] was used as the precursor in the synthesis of the target Pt(IV) compound.[44] Compound **1** was prepared by amide coupling of one of the succinate groups of [$Pt(NH_3)Cl_2(O_2COCH_2CH_2)_2$] with the free amine group in **4** (Scheme 2). Standard amide coupling protocols using reagents like EDC/NHS, PYBOP-HOBT, or DCC were unsuccessful. After several attempts, we determined that HATU/DIPEA could readily furnish **1** in 51% yield. The formation of **1** was confirmed by the presence of the parent ion peak at 1158.1 in the LC-MS (Figure S3).

In order to demonstrate the folate receptor targeting properties of **1**, we employed a FITC-labeled conjugate of folic acid (FA-PEG-FITC, **2**). This compound allowed us to determine whether a PEG-conjugated folic acid can interact with FR on the surface of a tumor cell by using fluorescence microscopy.

The synthetic route to **2** is given in Scheme 3. The mono-BOC-protected PEG amine (**3**) was coupled to FITC by a thiourea linkage to afford **5**, which was deprotected to give **6** containing a free amine. Conjugation of **6** to folic acid by amide coupling was performed by using the activated folate-γ-NHS ester in the presence of HATU/DIPEA to yield the final compound **2**.

In the next step we used noncovalently functionalized SWNTs having phospholipid-tethered amines on their surface. A polyethyleneglycol chain was introduced between the amine and phospholipid moieties to improve the solubility of the SWNTs and to keep functional groups away from the nanotube surface. The diameters and lengths of the functionalized SWNTs were 1−5 nm and 100−300 nm, respectively. Compound **1** was tethered to SWNTs by EDC/NHS amide coupling (Scheme 4).[29] Platinum atomic absorption spectroscopy (AAS) demonstrated that **1** can be easily attached to the functionalized SWNTs, which can carry a payload of around 82 Pt(IV) units per SWNT. This Pt(IV)−SWNT construct can deliver a significant dose of cisplatin selectively to FR(+) cancer cells, reducing side effects that are often exhibited by the platinum anticancer drugs, especially *cis*-DDP.

Redox Properties. Since reduction of Pt(IV) complexes inside the cell to release an active Pt(II) species is one of the key steps for their successful utilization in cancer therapy, we determined the reduction potentials of **1** at two different physiological pH values by cyclic voltammetry. An ideal situation for Pt(IV) reduction demands that it be sufficiently stable to travel through the body without decomposition until it reaches a tumor cell and that it have the appropriate reduction potential to be reduced only when inside the cell. Premature reduction in the bloodstream is a serious problem since it both sheds the axial targeting groups and produces a reactive Pt(II) that can become deactivated in plasma and/or produce detrimental side effects. Electrochemical studies of **1** at pH 7.4 and 6.0 revealed behavior characteristic of irreversible loss of the axial ligands. At pH 7.4, a value close to that in blood, the reduction potential of **1** is −0.698 V vs NHE. At a pH value of 6.0, closer to that in endosomes and lysosomes,[54–56] there is a positive shift by 126 mV in the reduction potential of **1** to −0.572 V vs NHE.

These potentials were obtained following extrapolation to a scan rate of 0.0 mV s^{-1} to account for the irreversible behavior of the reduction processes.[57] Irreversible cyclic voltammetric responses and the linear fits of potentials at different scan rates are presented in Figures S7−S10. Facilitated reduction at pH 6.0 is driven thermodynamically by protonation of the axial carboxylate groups as they depart the platinum coordination sphere. The acidic environment that builds up in and around cancer cells therefore facilitates Pt(IV) reduction. The reduction potential of satraplatin, a Pt(IV) compound currently in clinical trials, is −0.053 V vs

(51) Lee, R. J.; Low, P. S. In *Drug targeting: Strategies, principles, and applications*; Francis, G. E., Cristina, D., Eds.; Methods in Molecular Medicine *25*; Humana Press: Totowa, NJ, 2000; pp 69−76.
(52) Fan, J.; Pope, L. E.; Vitols, K. S.; Huennekens, F. M. *Biochemistry* **1991**, *30*, 4573–4580.
(53) Levy, C. C.; Goldman, P. *J. Biol. Chem.* **1967**, *242*, 2933–2938.
(54) Arunachalam, B.; Phan, U. T.; Geuze, H. J.; Cresswell, P. *Proc. Natl. Acad. Sci. U.S.A.* **2000**, *97*, 745–750.
(55) Collins, D. S.; Unanue, E. R.; Harding, C. V. *J. Immunol.* **1991**, *147*, 4054–4059.
(56) Kam, N. W. S.; Dai, H. *Phys. Status Solidi B* **2006**, *243*, 3561–3566.
(57) Nicholson, R. S.; Shain, I. *Anal. Chem.* **1964**, *36*, 706–723.

NHE.[58] The instability of satraplatin in blood has been a point of concern for many years. Its half-life of only 35.8 min in blood is a consequence of its relatively high reduction potential at pH 7.4. Compound **1** is expected to be much more stable in blood than satraplatin.

A comparison of the cathodic potentials of **1** at pH 7.4 with those reported for several Pt(IV) compounds is presented in Table 1. The cathodic reduction potential varies with the electron-withdrawing ability and bulkiness of the axial ligands.[59] The lowest reduction potential of **1** among the Pt(IV) complexes listed in Table 1 might be a consequence of the bulky folate ligand at an axial position.

Ability of 1 To Target and Destroy Folate Receptor-Positive Cancer Cells. The ability of SWNT-tethered **1** to destroy cancer cells was studied by using the MTT assay. To prove folate receptor-mediated targeting, we investigated FR-positive [FR(+)] human choriocarcinoma (JAR) and human nasopharyngeal carcinoma (KB) cell lines. FR-negative [FR(−)] testicular carcinoma cells (NTera-2) were used as a control (Figure 2, Table S1). Compound **1** and *cis*-DDP were examined as additional controls. The IC_{50} values are 0.019 and 0.01 μM, respectively, for SWNT-tethered **1** treatment of FR(+) JAR and KB cells, significantly lower than those of *cis*-DDP or **1**. The IC_{50} values for *cis*-DDP and **1** with KB cells are 0.086 and 0.15 μM, respectively. The IC_{50} value of SWNT−**1** increases to 0.048 μM with FR(−) NTera-2 cells, demonstrating targeted uptake by the FR(+) cells. In principle, comparison with JAR or KB cells in which the folate receptor had been eliminated, for example by RNA_i, would have been more appropriate, but such lines are at present not available to us. NTera-2 cells are, in our experience, among the most sensitive to cisplatin, however, so the comparison may be valid. The superior cell-killing ability of SWNT−**1** over **1** in FR(+) KB and JAR cells indicates that the SWNT longboats can deliver their platinum cargos containing a folate homing device selectively to folate receptors overexpressed on the cancer cells. The Pt(IV)−SWNT construct is >8 times more toxic to FR(+) cancer cells, a value that would be significant in a clinical context.

One of the important concerns in the design of conjugated systems is to ensure that the cytotoxic moiety, *cis*-DDP in this case, releases from the carrier and can reach its ultimate receptor, which is DNA in the cell nucleus in the case of *cis*-DDP. The reduction potentials together with the IC_{50} values demonstrate that our SWNT−**1** construct fulfills all the criteria.

Folate-Targeted Cell Uptake Studies of FITC-Labeled Folate Conjugate 2. The ability of a FITC-labeled conjugate of folic acid (**2**) to target FR(+) cells was evaluated by fluorescence microscopy. The results, summarized in Figure 3, clearly indicate that **2** selectively accumulates in the FR(+) KB cells (upper panel) when compared with uptake in FR(−) NTera-2 cells (lower panel). Compound **2** concentrates mainly in the cytoplasm of KB cells after 2.5 h of incubation at 37 °C. The conjugate **2**, having two moieties, FITC and folic acid, linked by a PEG linker was able to internalize by FRME, indicating that the folic acid moiety in **1**, which contains a Pt(IV) center connected to folic acid by a PEG spacer, is suitable for the FRME pathway.

We also investigated the intracellular localization of SWNT-tethered **1** by fluorescence microscopy. We cotethered a fluorescein-based fluorophore to our SWNT−Pt(IV) conjugate, and the results indicated the presence of fluorescent SWNTs in the endosomes, supporting the conclusion that uptake of SWNTs occurs through endocytosis (Figure S11).

Intracellular DNA Adduct Levels. To learn whether or not, once inside cells, platinum is released from SWNT or folate receptors, a platinum localization experiment was performed. Cytosolic and nuclear extracts were collected from KB cells incubated with 1 μM SWNT−**1** for 3 h, and platinum concentrations were determined by AAS. The nuclear fraction showed a considerable amount of platinum (86 ng of Pt/mg of protein). The level of platinum in the cytosol was comparatively less (11 ng of Pt/mg of protein). We did not observe any detectable amount of platinum in the cytosol or nucleus of cells treated with untethered **1** under similar experimental conditions. Not only was the cytotoxicity of the SWNT−**1** conjugate superior to that of **1**, but the latter also attained higher platination levels with nuclear DNA, clearly demonstrating that the *cis*-DDP moiety is efficiently released from the SWNT and receptor in the cancer cell environment.

Formation of Pt−1,2-d(GpG) Intrastrand Cross-Links. The major reaction product of *cis*-DDP with nuclear DNA is the 1,2-d(GpG) intrastrand cross-link, which occurs in >75% of all adducts. We employed monoclonal antibody R-C18,[50] which is specific for *cis*-DDP intrastrand 1,2-d(GpG) cross-links, to probe whether *cis*-DDP released from SWNT−**1** forms this adduct with nuclear DNA. In KB cells, after a 12 h treatment with SWNT−**1**, the presence of the 1,2-d(GpG) intrastrand cross-links was detectable by antibody-derived green fluorescence in the nuclei of the cells (Figure 4). The appearance of 1,2-d(GpG) intrastrand cross-links was also carried out using *cis*-DDP as a control (Figure 4). To our best knowledge, this is the first demonstration of 1,2-d(GpG) intrastrand cross-link formation with an active Pt(II) species formed upon reduction of a Pt(IV) precursor with nuclear DNA in a cell.

Conclusions

In this study, we introduce a route for preparing Pt(IV) complexes containing both a cell receptor targeting moiety and a delivery system. In particular, we established that **1**, containing a folic acid derivative as one of its axial ligands, specifically targets folate receptor-enriched tumor cells. Compound **1** has significantly enhanced cell-killing properties when conjugated to SWNTs, which facilitate its delivery via endocytosis. SWNT-tethered **1** is more active by a factor of 8.6 compared to cisplatin and, upon reduction in the cellular environment, it forms the major cisplatin 1,2-d(GpG) intrastrand cross-links with nuclear DNA. The internalization studies showed high and specific binding to the FR for the SWNT−**1** conjugate. Our data provide strong evidence that platinum−SWNT constructs containing a folate component will be valuable for targeted delivery of platinum anticancer agents. The modular nature of the synthetic approach and the ability of the longboats to carry 2 orders of magnitude greater platinum payloads per molecule than mononuclear complexes such as cisplatin or carboplatin should be valuable in future research.

(58) Choi, S.; Filotto, C.; Bisanzo, M.; Delaney, S.; Lagasee, D.; Whitworth, J. L.; Jusko, A.; Li, C.; Wood, N. A.; Willingham, J.; Schwenker, A.; Spaulding, K. *Inorg. Chem.* **1998**, *37*, 2500–2504.
(59) Ellis, L. T.; Er, H. M.; Hambley, T. W. *Aust. J. Chem.* **1995**, *48*, 793–806.

Acknowledgment. This work was supported by the National Cancer Institute under grants CA034992 at MIT and NCI-NIH-CCNE-TR at Stanford and by the Deutsche Forschungsgemeinschaft under grant TH 251/5-1 to J.T. S.D. is thankful to the Anna Fuller Fund in molecular oncology for a postdoctoral fellowship. We thank Dr. Elisa Tomat for preparing 6-carboxy-2′,7′-dichlorofluorescein-3′,6′-diacetate succinimidyl ester. We thank Dr. Katie R. Barnes and Ms. Caroline Saouma for initial studies in our laboratory toward the goals of this article.

Supporting Information Available: ^{1}H, ^{195}Pt, and ESI-MS spectral data of **1** (Figures S1−S3), HPLC analysis (Figure S4) and ESI-MS (Figure S5) for **2**, CPG hydrolysis of **4** (Figure S6), cyclic voltammograms of **1** (Figures S7−S10), a fluorescence microscope image of fluorophore-tethered SWNT−**1** (Figure S11), and a table of IC_{50} values (Table S1). This material is available free of charge via the Internet at http://pubs.acs.org.

JA803036E